Journal of the Korean Nuclear Society
Volume 4, Number 4, December, 1972

≪Original≫

Study of the Molecular Reorientation in Ammonium Sulfate by Neutron Scattering

Huhn Jun Kim

Physics Division, Atomic Energy Research Institute, Seoul, Korea

(Received October 17, 1972)

Abstract

Molecular reorientation in $(NH_4)_2SO_4$ has been studied by cold neutron scattering. For T=300°K data, the isolated quasielastic spectra and form-factors at various scattering angles are compared with four reorientational models based on SKÖLD theory. From these, it is concluded that the NH_4 ions are performing either 3-fold four axes or 2-fold three axes reorientation with $\tau_c=2.0\times10^{-11}$ sec. The temperature dependence of τ_c is studied over 100°K−413°K and for the high-temperature phase, the widths of composite spectra are compared with the results from NMR relaxation measurements. All the results have shown that the neutron scattering method is capable of giving detalis of the reorientational modes in solids and therefore some discussions are given on the application of this method. A study of the form-factor is applied for NH_4I (phase I) by comparing the measurement with the calculation based on free rotation approximation and proposed a reorientation model of NH_4 ions in the octahedral potential cage with $\tau_c\lesssim10^{-12}$ sec. Also a brief theoretical prediction for the effect of reorientational motions on the inelastic spectrum is discussed.

요 약

中性子散亂을 이용하여 $(NH_4)_2SO_4$에 있어서 分子의 再配向(reorientation)을 조사하였다. T=300°K의 測定에 대해서는 여러散亂角度에서 分離된 準彈性散亂스펙트럼과 構造因子(form-factor)를 SKÖLD 理論에 의한 네개의 再配向模型과 비교하여 NH_4 이온이 $\tau_c=2.0\times10^{-11}$sec 인 3重回轉 4軸(3-fold four axes) 또는 2重回轉 3軸再配向을 한다는 결론을 얻었다. τ_c의 溫度依存性을 100°K−413°K에 걸쳐 조사했으며, 高溫相에 대해서는 複合스펙트럼의 幅을 NMR 弛緩時間測定에 얻은 결론과 비교하였다. 이상의 결과는 中性子散亂이 固體에 있어서 分子再配向의 상세한 조사에 有力한 方法임을 보여 주었으며 따라서 이 方法의 應用에 대한 고찰을 하였다. 그 한 예로서 NH_4I(相 1)에 대해서 測定한 彈性構造因子와 自由回轉近似에서 얻은 理論値를 비교하여 NH_4 이온이 8面體型포텐샬(Potential)에서 $\tau_c\lesssim10^{-12}$sec 인 再配向을하고 있음을 주장하였다. 分子再配向이 非彈性스펙트럼에 미치는 영향에 대하여 간단한 理論的考察을 하였다.

1. Introduction

The techniques of neutron scattering have been used by many workers in the study of the rotational behavior of molecules. Particularly for solids, most of these methods involve basically study of (1) the torsional or rotational level structure measured by neutron inelastic scattering cross section or subthermal neutron total cross section and (2) the proton "thermal cloud" by elastic from-factor. However, none of these methods can directly detect the molecular reorientation.

In general, the molecular reorientation is low-frequency motion in atomic scale. From the uncertainty principle between time and energy, it follows that this long time behavior yields the small energy transfer (quasielastic scattering) spectrum and accordingly causes the elastic peak apparently broadened. In contrast with the extensive study of various diffusive motions in liquids by the quasielastic scattering of cold neutron, study of these effects in crystalline phases has started recently. The molecular reorientations in pentane, pentanol[1] and also in some globular compounds[2] have been performed. In those studies, theories for the solid phase are treated as the limiting case of those for the liquid phase. On the basis of the *jump-diffusion* model in liquids[3], SKÖLD[4] has attempted a simple reorientational behavior through distinct angles to interprete the quasielastic broadening observed in incoherently scattered neutron spectrum from solid methane. In his work, the reorientational modes have been deduced from the widths of composite peaks and the result is of a qualitative nature. Similar study has been carried out for solid neopentane by LECHNER *et al*[5].

Based on SKÖLD model, this paper presents the results of cold neutron experiment on $(NH_4)_2SO_4$ designed to study the reorientational mode of NH_4 ions. Making use of an advantageous instrumental resolution, comparisons can be made in improved way between observed results and proposed reorientational models. The results showed that simple reorientational behavior can explain observations fairly well and thus some discussions are extended to its applications in view of this method being still in exploratory stage.

It has been known that $(NH_4)_2SO_4$ undergoes a ferro-electric transition at $T_c=244°$ K with large transition entropy($\Delta S=4.2$ cal/mol·deg), changing from a structure in space group P_{nam} to P_{na} 2, There are two crystalographically independent groups of fonr NH_4 ions in the unit cell of both phases. Extensive studies have been done on this compound using various spectroscopic techniques. However, the nature of transition is not yet clear and there is sharp disagreement between the neutron diffraction[6] and NMR[7] works. According to the former, the transition results in stronger hydrogen bonds and less distortion of NH_4 ions in low-temperature phase, whereas the latter has proposed an order-disorder mechanism of the NH_4 ion tetrahedra with respect to the crystal *ab* mirror plane. The latter work has also pointed out that the reorientation of NH_4 ions could possibly proceed rotations around either 3-fold or 2-fold axes. Due to its complexity, detailed crystal structure of this compound is not considered for the model calculations in the present work.

2 Theory

Since neutron scattering by $(NH_4)_2SO_4$ is predominantly from protons and incoherent, only this contribution is considered here. VAN HOVE[8] has shown that incoherent differential scattering cross section is given by

$$\frac{d^2\sigma}{d\Omega d\omega}=N\frac{K}{K_o}\sigma^2_{\text{inc}}\,S_{\text{inc}}(\boldsymbol{Q},\omega), \qquad (1)$$

where σ_{inc} is the bounded incoherent scatter-

ing length and N is the total number of protons in the scattering system. The momentum and energy transfer are related to the initial and final wave vectors $\boldsymbol{K}_0$ and $\boldsymbol{K}$ through the relations

$$\boldsymbol{Q}=(\boldsymbol{K}-\boldsymbol{K}_0);\quad \hbar\omega=\frac{\hbar^2}{2m}(K^2-K^2_0), \qquad (2)$$

m being the neutron mass. Following VAN HOVE, the incoherent scattering function can be written more specifically as the Fourier transformation of self space-time correlation function $G_s(r,\ t)$ over the momentum and energy transfer as follows,

$$S_{inc}(\vec{\boldsymbol{Q}},\ \omega)=\frac{1}{2\pi}\int d^3r\int_{-\infty}^{\infty}dt \exp\left[i(\boldsymbol{Q}.\boldsymbol{r}-\omega t)\right]\cdot G_s(r,t). \qquad (3)$$

In the classical limit, $G_s(r,\ t)$ defines the probability density for finding a particle in the unit volume at r at time t, if at $t=0$, the same particle was at the origin r_0.

As can be seen from Eqs. (1) and (3), the complete information about the dynamics of the scattering system will, in principle, be obtained in the form of $G_s(r,\ t)$, if the inverse Fourier transformation of the experimental data can be made over the complete ranges of ω and $\boldsymbol{Q}$. Unfortunately the data are seldom complete enough for such a procedure and one has to resort to more indirect methods. By making use of its simple physical content in the classical limit, these usually involve the phenomenological calculation of $G_s(r,\ t)$ based on simple models with adjustable parameters which can be compared to the experimental data after Fourier transformation. The information obtained in this way is contained in the values of the parameters that give the best fit to the observations.

In solid, the NH_4 ion situated in a potential well will execute various modes of thermal vibration about its equilibrium position and once in a while the ion may rotate itself to other equilibrium orientations around the axes, tunneling most probably the minimum barrier to rotation. Let us assume that the quasi-elastic broadening is caused by the frequent reorientations of the molecule and again assume that the reorientation is uncorrelated with the thermal vibrations. In this case, ignoring the inelastic part, the scattering function can be written

$$S_{inc}(\boldsymbol{Q},\ \omega)=e^{-2W}S_R(\boldsymbol{Q},\ \omega), \qquad (4)$$

where $S_R(\boldsymbol{Q},\ \omega)$ describes the scattering function due to the reorientational effect only. e^{-2W} is well known Debye-Waller factor with the relation

$$2W=Q^2\langle r^2\rangle/3=Q^2(\langle r^2_t\rangle+\langle r^2_r\rangle+\langle r^2_i\rangle)/3, \qquad (5)$$

where $\langle r^2_t\rangle$, $\langle r^2_r\rangle$ and $\langle r^2_i\rangle$ are the mean square displacements of the proton from its equilibrium position due to isotropic translational, torsional and internal vibrations, respectively.

As mentioned already, SKÖLD has introduced a simplified reorientational behavior summarised as follows;

(a) The reorientational jump takes place very rapidly compared to the mean time between successive reorientations τ_c so that the reorientational jumps can be considered to be instantaneous and therefore the proton is always at one of the equilibrium sites.

(b) The reorientation occurs with equal probability around all of the allowed axes of the tetrahedral molecule.

In these cases, the classical correlation function is given as

$$G_R(r,\ t)=\sum_i P_i(t)\cdot\delta(r-r_i), \qquad (6)$$

with summation over all possible sites. $P_i(t)$ is the conditional probability for finding a proton at r_i at time t, given that it was at r_0 at $t=0$, and can be obtained by solving the differential equations for the fractional

population in each site;

$$\frac{\partial P_i(t)}{\partial t}=\tau^{-1}\left[n^{-1}\sum_{j=1}^{n}P_j(t)-P_i(t)\right]. \quad (7)$$

Here the summation is over n sites from which the proton can jump to site i and τ^{-1} is the mean jumping rate of one proton from one site to another. The solutions of Eq. (7) depend only on the model which one assumes for the reorientation of NH_4 ions. The experiment was carried on the polycrystalline sample and therefore $S_R(\boldsymbol{Q}, \omega)$ should be averaged over all possible orientations of the crystallites with respect to $\boldsymbol{Q}$.

The followings are the calculated results for the four simple reorientation models which one can consider likely to occur mainly for steric reason of NH_4 ion with its tetrahedral structure rather than the detailed crystal structure of $(NH_4)_2SO_4$.

(a) 3-fold four axes reorientation: (model A)

In this model reorientation of NH_4 ion takes place through 120° jump about its four 3-fold axes. Putting $\tau=4\tau_c/3$, SKÖLD has shown

$$S_R(Q, \omega)=(1+3B)\cdot\delta(\omega)+\frac{3}{\pi}(1-B)\,L(\tau_c^{-1}), \quad (8)$$

with $B=\dfrac{\sin QR_2}{QR_2}$,

$$L(\tau_c^{-1})=\frac{\tau_c^{-1}}{\omega^2+(\tau_c^{-1})^2},$$

and $R_2=1.83$Å[6] is the H-H distance.

(b) 2-fold three axes reorientation: (model B)

The reorientation of 180° about three 2-fold symmetry axes gives the same result as the model A.

(c) 3-fold uniaxial reorientation: (model C)

According to neutron diffraction work[6], one of the NH_4 ion groups in $(NH_4)_2SO_4$ has a considerably shorter N—H·····0 bond than others in both phases and it would be also plausible to consider the possibility of 3-fold uniaxial reorientation of NH_4 ion around only this N-H axis with the strongest hydrogen bonding. Putting $\tau=\tau_c$ and $\sum_1^3 P_i(t)=1$, this model gives

$$S_R(Q, \omega)=(1+1+2B)\cdot\delta(\omega)+\frac{2}{\pi}(1-B)\cdot L\left(\frac{3}{2}\tau_c^{-1}\right). \quad (9)$$

In this equation the additional unity in the parenthesis of the first term comes from the allowance of a stationary proton of NH_4 ion.

(d) 4-fold three axes reorientation: (model D)

The reorientation through 90° jump around three 4-fold symmetry axes is assumed. In this case the fractional population is given by different equation for each site which has different jumping environment with respect to the origin r_0, *i.e.*

$$\begin{aligned}
\frac{\partial P_0(t)}{\partial t}&=\tau^{-1}\left[P_1(t)-P_0(t)\right],\\
\frac{\partial P_1(t)}{\partial t}&=\tau^{-1}\left[\frac{P_0(t)+2P_2(t)}{3}-P_1(t)\right],\\
\frac{\partial P_2(t)}{\partial t}&=\tau^{-1}\left[\frac{2P_1(t)+P_3(t)}{3}-P_2(t)\right],\\
\frac{\partial P_3(t)}{\partial t}&=\tau^{-1}\left[P_2(t)-P_3(t)\right],
\end{aligned} \quad (10)$$

where subscripts 1, 2 and 3 denote the first, second and third nearest site from the origin respectively. Solving these equations simultaneously under conditions $\tau=\tau_c$, $P_0(0)=1$ and $P_0(t)+3P_1(t)+3P_2(t)+P_3(t)=1$, and proceeding similar calculations, one finds

$$\begin{aligned}
S_R(Q, \omega)=&(1+3A+3B+C)\cdot\delta(\omega)\\
&+\frac{1}{\pi}\left[3(1-A-B+C)\cdot L\left(\frac{1}{3}\tau_c^{-1}\right)\right.\\
&+3(1+A-B-C)\cdot L\left(\frac{2}{3}\tau_c^{-1}\right)\\
&\left.+(1-3A+3B-C)\cdot L(2\tau_c^{-1})\right], \quad (11)
\end{aligned}$$

with $A=\dfrac{\sin QR_1}{QR_1}$, $B=\dfrac{\sin QR_2}{QR_2}$,

$$C=\frac{\sin QR_3}{QR_3}.$$

Here $R_1=R_2/\sqrt{2}$ and $R_3=\sqrt{3}R_1$ are other intermolecular H-H distances.

All the above results show that the spectrum of incoherently scattered neutrons from the molecule reorientating between equivalent or non-equivalent configurations consists of two parts, namely, elastic and quasielastic. Of these, the elastic part is governed by the asymptotic proton behavior at $t\to\infty$. Since at infinite time the protons concerned can occupy different equivalent sites, the elastic scattering has associated with it a form-factor which describes the diffraction from the structure of the proton distribution. On the other hand, the quasielastic part is controlled by the time evolution of the reorientation. While the angular variation of the intensity is determined (as with elastic scattering) by the geometry of the reorientation process, the shape of the spectrum is characterized by Lorentzian form and its width is related only to the rate of reorientation τ_c^{-1} and not Q-dependent due to the assumption of instantaneous jumping mechanism.

3. Experimental Method

All the measurements were carried out by the time-of-flight method using high resolution rotating crystal spectrometer installed at CIRUS reactor in Bhabha Atomic Research Centre. Fig. 1 shows the schematic drawing of the spectrometer.

A collimated beam from the reactor after being passed through the single crystals of lead and quartz to reduce fast neutron and gamma ray backgrounds is allowed to pass through a 10 cm thick polycrystalline beryllium filter to produce a cold neutron beam. The cold neutron beam is Bragg-reflected through an angle of $2\theta_m=126°$ by the (111) plane of a spherical aluminium single crystal of about 5 cm in diameter rotating at 8,000 rpm. The crystal rotor is driven by a hysteresis synchronous motor and a 400 Hz. power supply. The rotational speed does not change by more than $\pm 1\%$ in a daily run. Periodic two bursts of 4.87 meV (4.1 Å) neutrons per revolution obtained in this way are allowed to strike the sample placed 65 cm apart from the crystal rotor after being passed through a Soller slit collimator (divergence of ~2°) and a thin monitor counter.

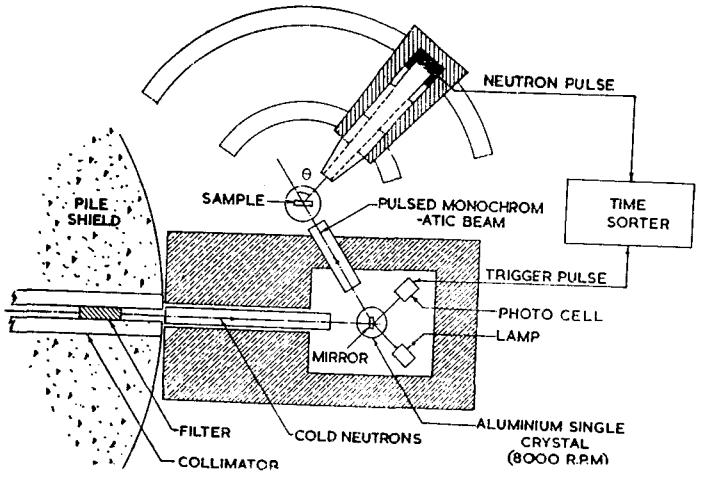

Fig. 1. Schematic drawing of the rotating crystal spectrometer.

The scattered neutrons traverse a flight path of 300 cm at the end of which they are detected by a set of six BF_3 detectors placed with its long axis perpendicular to the beam direction. Each detector is 5 cm in diameter and the solid angle subtended by these detectors at the center of the sample is 0.0075 steradian with the horizontal span of 6.5°. The entire assembly of flight tube and detector bank with its massive shield is mounted on a trolley and can be moved on tracks so that the scattering angle can be covered continuously over the range of 0°-101°.

The reference pulse for starting the timing circuits is obtained by the mirror with two faces fixed to the rotor shaft to reflect a light beam to a photocell each time the plane comes into reflecting position. Data are stored in a 512 channel time analyzer with 8 μsec channel width.

In order to monitor the sample transmission, the second monitor detector is placed on the transmitted beam path. The output signal from this monitor is fed to 3 channel time analyzer with 300 μsec channel width and triggered by the same time reference pulse. The distance between crystal rotor and the second monitor detector is so adjusted that the second channel counts the neutrons centered around the incident monochromatic neutron burst, while the first and third channels count the neutrons coming during the 300 μsec period before and after the second channel. Since the average count of the first and third channels is the background of the incident energy channel, the difference between the counts of the second channel and this background gives the correct incident beam intensity, and therefore the ratio of these intensities with and without the sample gives the sample transmission.

The sample, in the form of powder, was sealed in thin-walled aluminium casette and held transmission geometry with the orientation of the half the scattering angle. The thickness of sample was 1.6 mm and the transmission was in the range of 62%-80% depending on the scattering angle.

Sample temperature could be varied continuously from 100°K to 413°K by means of a conventional liquid nitrogen cryostat and control of electric current to the heating coil attached around the sample casette. Measurements at more high temperatures were not attempted since the sample decomposes at 470° K. Two copper-constantan thermocouples were attached at the top and bottom of the sample and temperature was recorded continuously. The uncertainty of the sample temperature was negligible from room temperature to higher. Due to the large sample dimension and simple arrangement of cold finger-heating coil system, however, the difference between two thermocouple readings was observed to be increasing as the sample temperature became lower and it was about 10 °K at the sample temperature of about 100 °K.

4. Results

Data were accumulated to obtain reasonable counting statistics over only the energy region of current interest and thus no details of inelastic peaks were seen. Fig. 2 shows a typical example of raw data at room temperature for the scattering angle $\theta=90°$. The characteristic feature of all other distributions is similar to this with a broad inelastic spectrum and an overriding elastic peak with significant quasielastic broadening in the both wings of the peak. The inelastic background was subtracted by interpolating a smooth curve between two wings of the peak as denoted by the dashed line in Fig. 2 After applying

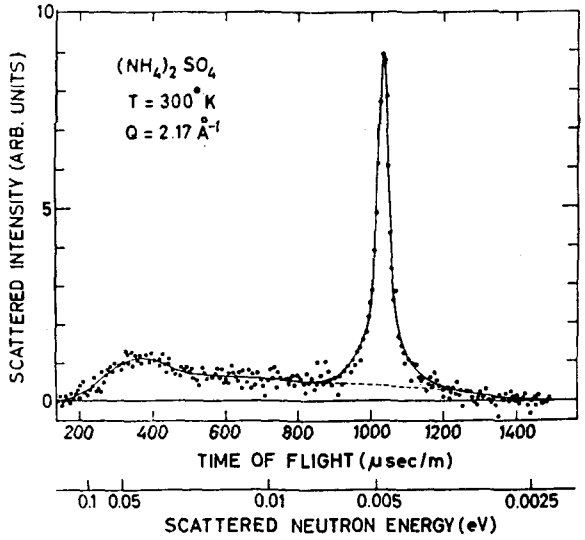

Fig. 2. A typical example of raw neutron time-of-flight spectrum with E_0= 4.87 meV and θ=90°.

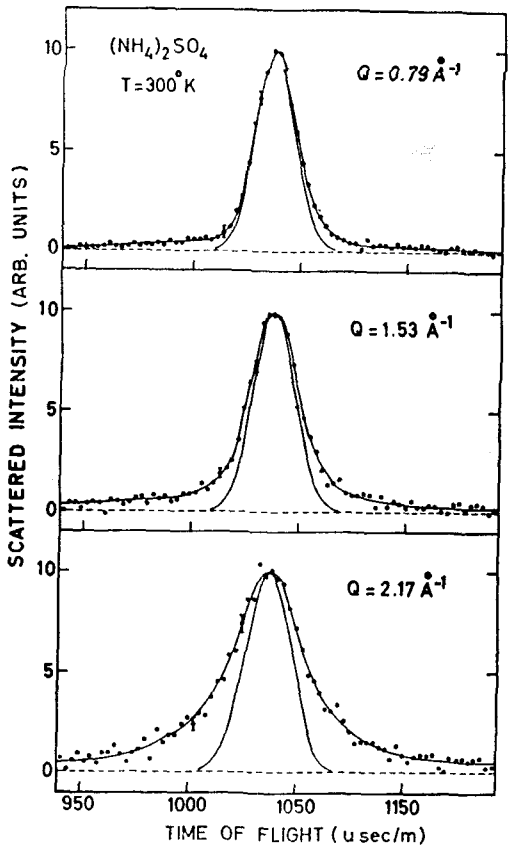

Fig. 3. Comparison of corrected composite peak distribution with related resolution function for three different mean wave vector transfers.

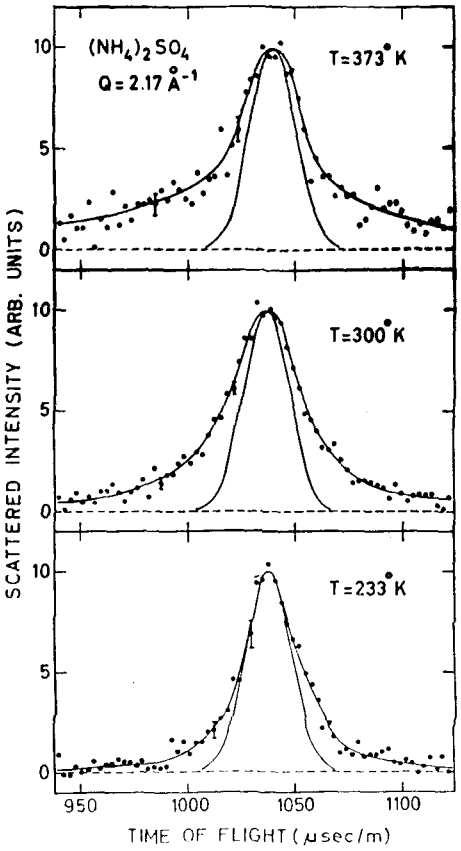

Fig. 4. Comparison of corrected composite peak distribution with resolution function at three different temperature.

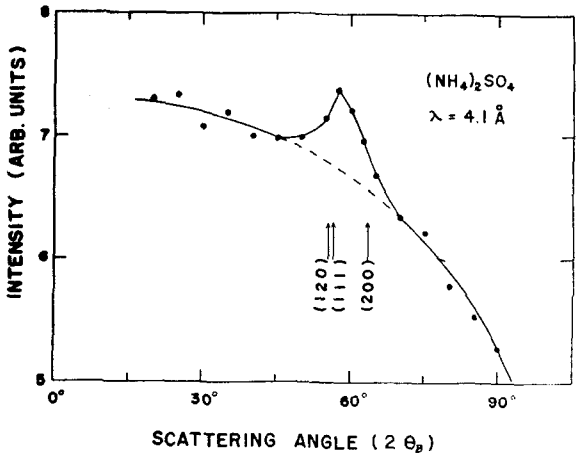

Fig. 5. Diffraction pattern measured from the sample in the half-angle transmission geometry. (θ_B: Bragg angle)

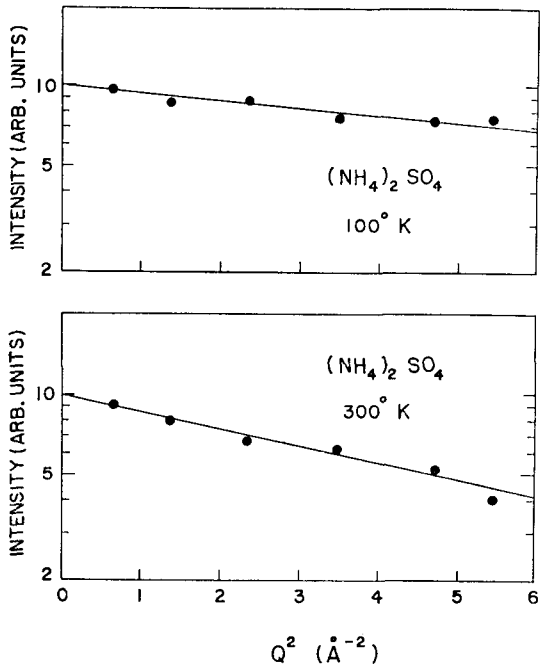

Fig. 6. Semi-log plot of the composite peak intensity *vs.* Q^2 at high- and low-temperature phases. The solid lines are least squares fit to the data

some standard corrections such as air out scattering and energy-dependent detector efficiency in the usual way, some typical distributions are shown in Fig. 3 and 4 where one can see that the quasiclastic broadening becomes more prominent at larger scattering angle and at increased temperature, the solid lines being the resolution functions.

Any influence of the coherent scattering on the data was checked by measuring the diffraction with the crystal rotor at stationary in the position of Bragg reflection and the sample at the half angle transmission position. The result shows that the data only at $\theta=60°$ has been affected by strong (120), (111) and (200) reflections[6] to some extent as seen in Fig. 5.

The angular dependence of the integrated peak intensity defined in the above manner gives information about the Debye-Waller factor. In Fig. 6, the semi-log plots of the integrated intensity against Q^2 are shown for the both phases, after applying normalization to the monitor counts and to the effective neutron beam cross-section in which the sample "sees". By fitting the straight lines using the weighted least-squares method, the results are $\langle r^2\rangle/3=0.054$ Å^2 at 100°K and $\langle r^2\rangle/3=0.143$ Å^2 at 300°K, respectively.

Simple theoretical estimate of $\langle r^2\rangle$ are made from the contribution of two components $\langle r^2_t\rangle$ and $\langle r^2_r\rangle$. As is the most cases with ammonium salts, the frequencies of internal vibration of NH_4 ion will be very high and, even for the lowest bending mode not many of these states will be excited at room temperature.

In the system of cubic symmetry, the Debye-Waller factor is given by[9]

$$2W=\frac{\hbar Q^2}{2M}\int d\omega\frac{g(\omega)}{\omega}\coth\frac{\hbar\omega}{2K_BT}, \qquad (12)$$

where $g(\omega)$ is the normalized frequency distribution and the other symbols have their usual meanings. For two components, if take Einstein approximations, Eq. (12) reduces to

$$2W=\frac{3Q^2\hbar}{2}\left(\frac{\coth\frac{\hbar\omega_t}{2K_BT}}{18M_H\omega_t}+\frac{\coth\frac{\hbar\omega_r}{2K_BT}}{4M_H\omega_r}\right), \qquad (13)$$

where M_H is the proton mass and the factors 18 and 4 in denominators are introduced for the effective masses of the translational and torsional modes respectively.

The optical and torsional peak frequencies[10,11] are assigned to be $\omega_t=29$ meV, $\omega_r=49.5$ meV at 100°K and $\omega_t=22.3$ meV, $\omega_r=38$ meV at 300°K, respectively. The value for ω_t at 300°K is estimated by extrapolating those frequencies at 100°K and 172°K. It is seen that thus estimated values $\langle r^2\rangle/3=0.045$ Å^2 at 100°K and $\langle r^2\rangle/3=0.112$ Å^2 at 300°K are in reasonable agreement with observed values.

For the comparison of the observed distributions to the theory, it is necessary to correct the instrumental resolution using the equation

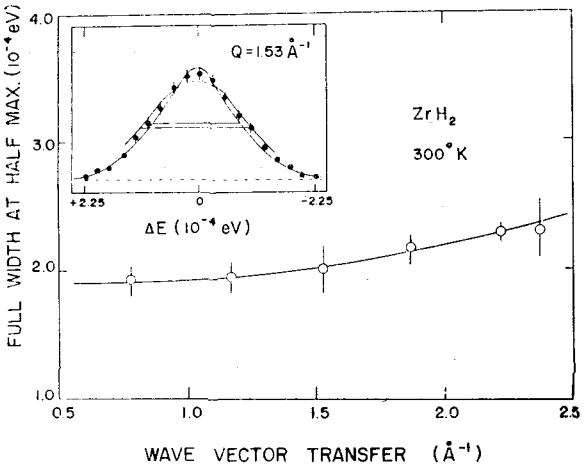

Fig. 7. Measured resolution width (FWHM) *vs.* Q. The inset shows the Gaussian nature of measured resolution function and also the way for the estimation of the width uncertainty.

$$S'(Q,\ \omega)=\int S(Q,\omega-\omega')\ R(Q,\omega')d\omega', \quad (14)$$

where $R(Q,\ \omega)$ stands for the resolution function The elastic resolution functions were determined from a series of measured distribution of the elastic incoherent scattering by ZrH_2 kept in same sample geometry to those of $(NH_4)_2SO_4$. All the distributions were observed to be Gaussian shaped, if neelect a small systematic deviation in the region of wings. The full width at half maximum of the resolution function against Q is presented in Fig. 7. The error bar shows the uncertainty of the width estimated by drawing smooth curves which give maximum and minimum widths within the counting statistics as shown in inset. The same method was adopted elsewhere in this work for the estimation of width or shape uncertainty. By fitting a smooth curve, it is seen that the energy resolution varies from 0.19 meV (20.2 μsec/m) to 0.23 meV(24.4 μsec/m) as Q varies from 0.79 Å^{-1} (θ=30°) to 2.37 Å^{-1}(θ=101°). Instead of the measured scattering function itself, $R(Q,\omega)$ was approximated by Gaussian form with the width obtained in this way for the

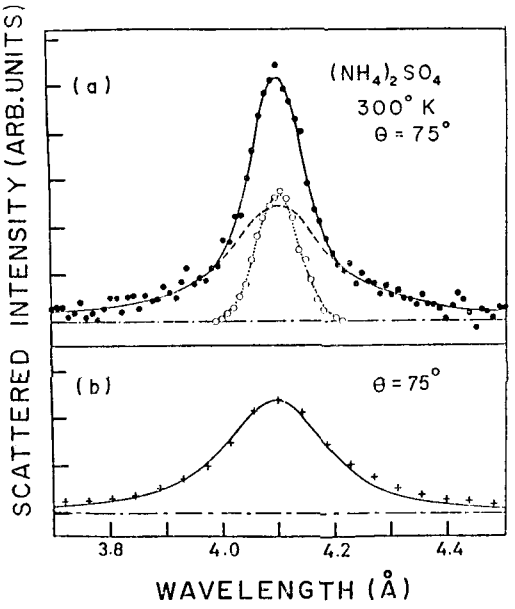

Fig. 8. (a) A typical example for the decomposition of the composite spectrum (solid dots) into two parts. The open dots show the measured resolution function. (b) Comparison of the isolated quasielastic spectrum (crosses) with model A or B (solid line) for $\tau_c=2\times10^{-11}$ sec.

data analysis to avoid undue complication.

The resolution correction can be accomplished either by unfolding the quasielastic part after isolating the elastic peak, or directly comparing the measured spectrum to the theoretical cross section folded over $R(Q,\ \omega)$ using Eq. (14). Although the former, of course, may introduce errors due to the statistical uncertainties in the observed points, it is expected that more informations (such as, form-factor) can be deduced from this procedure regardless of any prerequisite theory.

All the measured room temperature spectra were isolated graphically into two parts. This was done by first extrapolating the wings smoothly to obtain a reasonable representation of the quasielastic part as denoted by the dashed line in Fig. 8(a), where the spectrum at θ=75° is shown as an example. This separation was then adjusted by trial and error

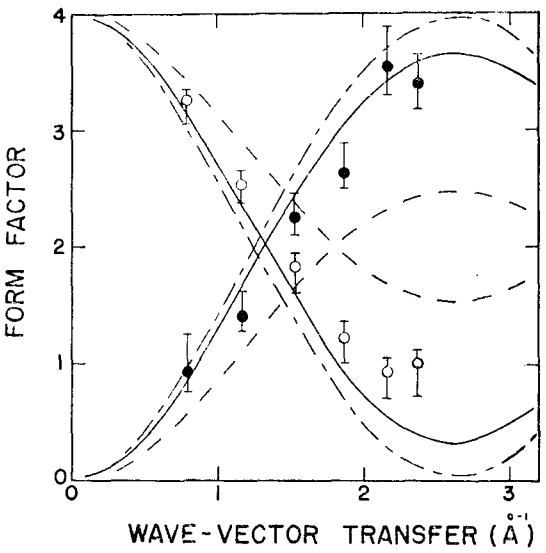

Fig. 9. Comparison of the elastic (open circles) and quasielastic (solid circles) form-factors with model A or B (solid lines), model C (dashed lines) and model D (brocken lines).

such that when subtracted from the total spectrum (solid line), the resulting curve (dotted line) matched closely to $R(Q, \omega)$ (open circles). In Fig. 8(b), the best estimate of the quasielastic part isolated in this way is shown by crosses.

Using three models, a large number of theoretical quasielastic distributions were computed for various τ_c and then folded over $R(Q, \omega)$. The comparison of those distributions with isolated quasielastic spectra showed that the result from model A (or model B) was fitted reasonably well when $\tau_c = 2.0 \times 10^{-11}$sec, as demonstrated by the solid line in Fig. 8(b). Similar results were obtained for all data at different scattering angles confirming that reorientations produce their own characteristic Lorentzian type spectra based on model A.

In Fig. 9, the intensities (areas) of the elastic and quasielastic parts (corrected for the Debye-Waller factor obtained experimentally) are plotted against Q. The area uncertainty introduced in the procedure for isolating is quite involved to estimate and therefore the error bars shown are based on the estimated shape uncertainty of the composite spectra alone. A comparison with the computed form-factors according to three different models shows that model A or model B (solid line) can be also chosen as the best possible fit, even though there is some disagreement quantitatively.

It is worthwhile to point out here that the form-factor study is usful in getting information about the modes of reorientation even without knowing the reorientation rate. For example, the model C (dashed line) can be easily ruled out. in Fig. 9 Further discussion on this respect will be seen in Sec. 5.

The temperature dependence of the scattering was studied to examine the effect produced by the variation of τ_c on the spectra. For the all spectra, if one can isolate elastic peak and quasielastic peak and plot resolution-unfolded quasielastic widths in the unit of ln τ_c against 1/T, informations on the potential barrier to the rotation V and pre-exponential factor τ_0 can be extracted by fitting a straight line assuming the relation

$$\tau_c = \tau_0 \exp(V/K_B T). \qquad (15)$$

For the decomposition, however, difficulty was experienced near T_c due to undistinguished broadening as will be seen the reason in Sec. 5. Thus, as far as these studies are concerned the most conveniently monitored quantity is the width of the composite spectrum. The measurements were best made at an angle where the ratio of the quasielastic to the elastic intensity is large. The full widths at half-maximum of the spectra as a function of T are shown in Fig. 10 for $\theta = 90°$. From the earlier results, a comparison is preferably made for model A using Eqs. (8), (14) and (15). Assigning τ_0 and V to be 3.14×10^{-13} sec and 2.3 kcal/mole respectively,

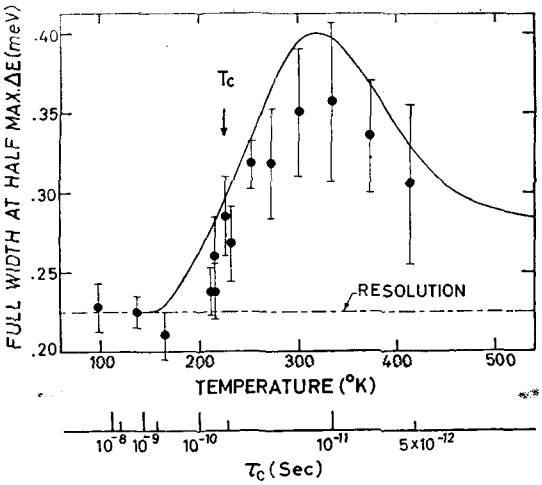

Fig. 10. FWHM of the composite spectrum *vs.* T for $\theta=90°$. (T_c: transition point) The solid line is the width predicted from model A or B using $\tau_0=3.14\times10^{-13}$ sec and V=2.3 kcal/mole. The lower scale shows the variation of τ_c *vs.* T.

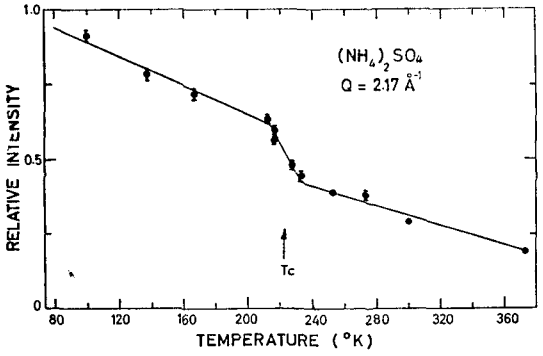

Fig. 11. Composite peak intensity *vs.* temperature.

these being the values deduced from NMR relaxation measurements[7], the resulting width distribution is shown as a solid line. According to NMR study, the parameters τ_0 and V change suddenly at T_c leading to the large value of τ_c at low-temperature phase. Therefore, if use more accurate parameters for the computation in this range, the solid line will decrease rapidly to the resolution at T_c giving rise to improved agreement between two observations. In view of the above, it can be seen that once again model A (or model B) is able to reproduce basically the same feature of the observed distribution. More significantly, they demonstrate the direct comparison that can be established between NMR and neutron scattering results.

5. Discussion

From the comparison of the experimental results with proposed models, it may be judged that the quasielastic spectra observed in $(NH_4)_2SO_4$ can be interpreted in good approximation due to the reorientation of NH_4 ions in terms of model A or model B. As regards these two models, no preferable choice can be made easily unless the surrounding potential well is very simple symmetry. Some quantitative disagreements between experiments and theory are to be anticipated, since in the complicated crystal field like $(NH_4)_2SO_4$ the reorientational behavior may be not so simple as assumed. Two independnt NH_4 groups may reorient with somewhat different rate and similar argument can be made also for all the allowed axes of reorientation. Also the effect of multiple scattering, which was disregarded in view of the fact that the energy transfer concerned in the analysis of data is small, may be not trivial with the sample transmission of 62%~80%.

An anomalous change of the composite peak intensity is observed at T_c (Fig. 11), as also reported by others[11]. What cause this anomaly is probably "softening" of the torsional oscillations of NH_4 ions, and may be understood qualitatively as follows; If the torsional frequency distribution changes significantly at T_c giving rise to more population in lower states at high-temperature phase, then there is an increase in probability of inelastic scattering with energy-gain experiment and an abrupt decrease in the elastic peak intensity.

From the slope of total scattering cross

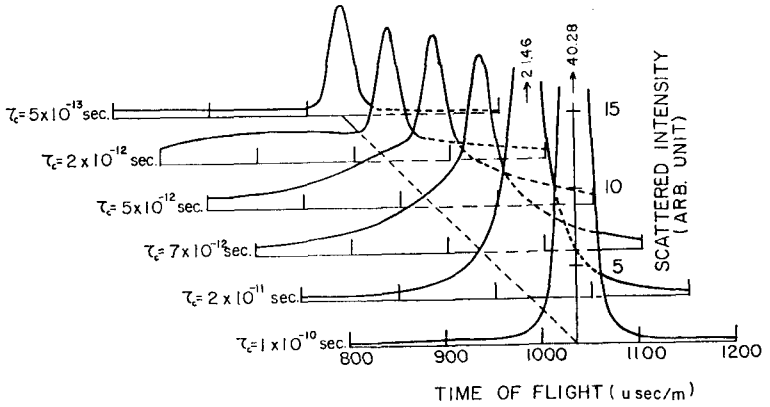

Fig. 12. Demonstration of the computed time-of-flight spectra based on model A and NH_4^+ tetrahedra for various τ_c.

section versus temperature ($\Delta\sigma_s/\Delta T/H$ atom), LEUNG *et al.*[12] have derived the average barrier heights of $(NH_4)_2SO_4$ and other ammonium salts. The basic idea of their work is also to reflect the change of torsional or rotational energy level structures sensitively on the total scattering cross sections using very low energy neutrons (1.13 meV) comparable to the rotational constant of NH_4 ion ($B=5.9cm^{-1}$). Seeing their remarkable results and a sensitive change of the composite peak intensity at T_c in this work, it can be suggested that the study of temperature dependence of composite peak intensities or pure elastic peak intensities may be explored as a potential method to derive the average barrier heights in similar way, even using Be-filtered neutrons.

It will be worthwhile to have some more discussion for the application of SKÖLD's model. According to his theory, the width of the quasielastic peak is related to the rate of reorientation alone. At high temperature when the rate is very high, the quasielastic spectrum will be considerably broadened out and only the elastic peak, as modified by the instrumental resolution, will be seen. At the other extreme of very low temperature, the reorientations will be very slow causing the quasielastic part to merge with the resolution-modified elastic peak, and once again no quasielastic spectrum will be observed. In between these limiting cases, both components can be identified subject to the conditions of the experiment.

In Fig. 12, some computed examples are demonstrated in the time-of-flight presentation over the range $\tau_c=1\times10^{-10}$sec to 5×10^{-13}sec, based on the model A and $\theta=90°$. From this, it can be seen that the range of experimentally observable broadening is limited approximately over the range of $\sim10^{-10}$ sec$>\tau_c>\sim10^{-12}$sec, unless measurements are carried out with better resolution. Of course, this range is also subject to the molecular size.

The instantaneous reorientation model is strictly valid when the reorienting time is much shorter than τ_c as being the bounded oscillatory time. However, if consider the cold neutron spends $\sim10^{-13}$ sec to travel over the order of correlation range, this simplification will break down when τ_c approaches to $\sim10^{-13}$ sec, because it is unrealistic to assume that the reorienting time of molecule is much shorter than the thermal vibrations of molecule ($\sim10^{-13}\sim10^{-14}$sec). For the rigorous theoretical formulation based on the classical limit, however, difficulty will arise because

the proton cloud due to the thermal vibrations is not fully developed during τ_c and accordingly the assumption of uncorrelation between the thermal vibrations and the reorientational motion is much more severe. As pointed out earlier, the elastic form-factor $F_s(Q)$ reflects information conveniently in this stage since the quasielastic part has become well washed out. $F_s(Q)$ which describes the diffraction from the structure into which the proton is distributed can be written in general form[13]

$$\left(\frac{d\sigma}{d\Omega}\right)_{\omega=0} \propto F_s(Q) = \left| \int d^3r \ \rho_\infty(r,t)\, e^{iQ\cdot r} \right|^2 \qquad (16)$$

where $\rho_\infty(r,t)$ denotes the proton density distribution at $t\to\infty$. In particular, if the occupation probabilities are equal for the all possible discrete sites, ignoring the effect due to thermal vibrations, Eq. (16) becomes

$$F_s(Q) = \left| \sum_i e^{iQ\cdot r_i} \right|^2 \qquad (17)$$

It can be seen that the space average of Eq. (17) reduces to the elastic form-factors in Eqs. (8), (9) and (11). when applied to the proposed reorientation modes in Sec. 2 In favorable cases the study of $F_s(Q)$ can lead to information about the size and shape of $\rho_\infty(r)$ and thereby about the mode of molecular reorientation without regard to τ_c. Moreover, applied to single crystal this method can help to show up anisotropic aspects of $\rho_\infty(r)$ sensitively.

For some of ammonium and methyle compounds, neutron inelastic scattering measurements show only abroad spectrum without any appearance of sharp peak at high-temperature phase. With regard to torsional peak, its disappearance has been explained on the basis of the free rotation or slightly hindered rotation of NH_4 ion or CH_3 group. One of the well known examples is NH_4 I (phase I) for which the free rotation and

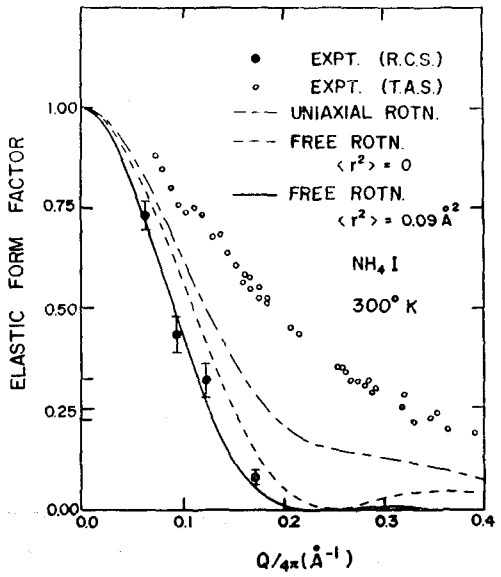

Fig. 13. Comparison of the elastc form-factors with those based on theoretical models.

uniaxial rotation models are proposed respectively by STEPHENSON *et al.*[14] and PLUMB *et al.*[15] from experimental evidences other than neutron spectroscopy. As an application of the form-factor study, the spectrum of this compound is measured at 300° K in similar way to $(NH_4)_2SO_4$ but with increased sample transmission of 37%-48%. The elastic peak shapes are observed to remain same as the resolution function. In Fig. 13 the angular variation of the elastic peak intensity is shown by solid dots in the data reported by VENKATARAMAN *et al.*[13] The error bars are those due to counting statistics and estimated intensity uncertainty at $Q=0$. Also shown with open dots are measurements by them using a triple axis spectrometer, while the dashed and broken curves are their theoretical form-factors based on the free rotation and uniaxial rotation models. As to the latter case, the effect due to the thermal vibrations is taken into account. One of the ways to give an account of the drastic disagreement between two observations can be made by

assuming very rapid reorientation of NH_4 ions in this phase. According to RUSH *et al.*,[16] the potential barrier to rotation in NH_4I (phase I) is about 0.5 kcal/mol which is comparable to K_BT. Therefore it seems unlikely to assume the free motion but much hindered rotation. In NaCl type potential cage of this phase, one can imagine number of quasi-equilibrium orientations of the NH_4 ion. For example, there are 48 of those orientations with one of the N-H bonds directed towards the halogen ions. If assume that the NH_4 ion which was executing large amplitude torsional vibrations reorients to these orientations with $\tau_c \lesssim 10^{-12}$ sec as suggested by PALEVSKY[17] from the neutron inelastic spectrum, the quasielastic part is to be completely broaden out in the present measurement with high resolution, while this broadening is not sensitive enough to be resolved with the incident beam energy of 70 meV and the resolution of $\Delta E=12$ meV in the triple axis spectrometer experiment. For the theoretical prediction of $F_s(Q)$ based on the reorientation model, however, difficulty comes from the estimate of the Debye-Waller factor in which conceivably anharmonic and anisotropic natures of $\langle r^2_r \rangle$ will make the major contribution. In view of the better agreement between the observation and the free rotation model in which infinitely thin spherical proton distribution is assumed, somewhat improved treatment can be made by assuming that the allowance of translational and internal vibrations of NH_4 ion causes the proton shell to have a Gaussian smear in the radial direction. In this case Eq. (16) becomes

$$F_s(Q)=\left|A\int_0^\infty e^{-(r-r_0)^2/2\sigma^2}\frac{\sin(Qr_0)}{(Qr_0)}r^2dr\right|^2, \tag{16'}$$

where A is the normalization factor and the N-H distance $r_0=1.03$Å. By assigning $\sigma^2=\langle r^2_t\rangle+\langle r^2_i\rangle=0.09$Å^2 estimated by VENKATARAMAN *et al.*, the computed result shown as the solid curve in Fig. 13 gives better agreement. As far as the form-factor study is concerned, this free rotation approximation is not much unrealistic in view of the highly symmetrical nature of the quasi-equilibrium orientations in NaCl type phase and thus the above discussion may be treated as an argument in favour of the reorientation of NH_4 ions with $\tau_c \lesssim 10^{-12}$ sec rather than free rotation. Similar study will deserve for the other ammonium compounds[13] in which also non-Guassian nature of the Debye-Waller factors were observed with triple axis spectrometer suggesting considerable freedom of NH_4 ions.

Finally, atlhough the main emphasis of this work is on the quasielastic scattering, some discussion about the effect caused by the reorientational motion on the inelastic spectrum may be of additional interest. To facilitate the calculation, let us consider one-dimensional structure in which two harmonic potential wells are apart by x_0, and a Boltzmann particle which was bound in a potential well performing thermal motion for a mean time τ jumps to the other site. In this case, by substituting the space-time correlation function of the harmonic oscillator[18] for δ-functions in Eq. (6), one has the expression

$$G_R(x,t)=P_1(t)G_v(x,t)+P_2(t)G_v(x-x_0,t), \tag{18}$$

$$\text{with } G_v(x,t)=[\pi W(t)]^{-\frac{1}{2}}\exp[-x^2/W(t)],$$
$$W(t)=(2V_0/\omega_1)^2(1-\cos\omega_1 t).$$

Here ω_1 is frequency of the oscillator and $V_0=(2K_BT/M_P)^{\frac{1}{2}}$ is the thermal speed. Introducing solutions of Eq. (7) to $P_1(t)$ and $P_2(t)$, the space-time Fourier transformation of Eq. (18) gives

$$S(Q,\omega)=e^{-x}\left[\pi(1+e^{iQ_xx_0})\sum_{n=0}^{\infty}\{(2-\delta_{on}I_n(z).\right.$$

$$[\delta(\omega-n\omega_1)+\delta(\omega+n\omega_1)]\}$$
$$+(1-e^{iQ_xX_o})\sum_{n=0}^{\infty}\{(2-\delta_{on})I_n(z)[L(-n\omega_1,\tau)$$
$$+L(n\omega_1,\tau)]\}\Big]. \quad (19)$$

Here $I_n(z)$ is the modified Bessel function of the first kind, δ_{on} is the Kronecker delta and also the following abbreviations are used;

$$Z=\frac{1}{2}\left(\frac{Q_xV_o}{\omega_1}\right)^2,$$
$$L(\pm n\omega_1,\tau)=\frac{\tau^{-1}}{(\omega\pm n\omega_1)^2+(\tau^{-1})^2}.$$

This equation is similar to the scattering function of the classical oscillator[18]. However, the second summation in terms of Lorentzian function is new term arised from our assumption Eq. (18), and implies that the broadening occurs not only at the elastic peak but also at the inelastic peaks. This is an interesting result because no such a quantitative prediction has been made thus far. Recalling $Z\angle 1$ under most conditions, if one retains to one-phonon excitation in the first order approximation, Eq. (19) reduces more explicitly to

$$S(\boldsymbol{Q},\omega)=e^{-z}\Big[\pi(1+e^{iQ_xX_o})\Big[\delta(\omega)+\frac{z}{2}\delta(\omega-\omega_1)\Big]$$
$$+(1-e^{iQ_xX_o})\Big[\frac{2\tau^{-1}}{\omega^2+(\tau^{-1})^2}$$
$$+\frac{z}{2}\frac{\tau^{-1}}{(\omega-\omega_1)^2+(\tau^{-1})^2}\Big]\Big]. \quad (20)$$

Here the common factor $\exp(-z)$ is the Debye-Waller factor, V_0/ω_1 being the mean amplitude of the oscillator. The from-factors $[1+\exp(iQ_xx_o)]$ and $[1-\exp(iQ_xx_o)]$ will become similar forms obtained in Sec. 2, if space average is made. According to Eq. (20), the nature of broadening and apparently rapid decrease of intensity for an elastic peak can be also stated for inelastic peaks in an analogous way. In writing Eq. (18), it is simply assumed that the thermal oscillations at two equilibrium sites are in phase. Also, details of "jump out" and "jump in" positions are simply thermal averaged from the beginning. To discuss rigorously to what extent these simplifications may be justified is not simple and is outside of the scope of this work. However this result is physically consistent with the energy uncertainty arised from the "life time effect" of an oscillator.

With increasing temperature, those broadenings of torsional peaks and apparently rapid decrease of torsionol peak intensities have been observed for $(NH_4)_2SO_4$[10, 11] and some other ammonium compounds[19, 20, 21] in which NH_4 ions are believed loosely bounded. With regard to the broadening of torsional peak, it can be also ascribed to Doppler broadening. Because of complicated nature of instrumental resolution as well as inelastic scattering spectrum, it is very much involved to check experimentally whether Eq. (19) will eventually lead to quantitative prediction. With onset of phase transition or increasing temperature, the reorientational motion may eventually go into almost free rotation well overcoming the potential barrier. However there are also considerable number of ammonium compounds which exhibit only a broad inelastic neutron spectrum at room temperature, while the estimate of potential barriers deduced from other methods are comparable to the magnitude of sample temperature. For these compounds, therefore, it is suggestive that NH_4 ions are still in the stage of very frequent reorientation, say 10^{-13} sec$\angle\tau_c\lesssim 10^{-12}$ sec, and the inelastic peaks are broadened out due to reorientation and other superposed effects.

In summary, the study of quasielastic spectrum, $\Delta F(Q)/\Delta T$ and also $F_c(Q)$ can provide useful complement to the inelastic scattering experiment and other spectroscopic methods to obtain detailed informations on the rotational behavior of molecules. The instanta-

neous reorientation model, even with its great simplification, offers a good approximation when molecules are performing reorientations through distinct angles in crystalline phase up to $\tau_c \sim 10^{-12}$ sec.

Acknowledgement

The auther wishes to express his most sincere gratitude to Prof. B. N. SUNG for his guidance and help during the course of this work. Thanks are also due to Dr. K. SKÖLD for helpful correspondence, and Prof. H. I. BAK for several useful discussions on the results.

Finally, it is a great pleasure to acknowledge the members of neutron scattering group at BARC for the continued support of this work, and especially Drs. P. K. IYENGAR, G. VENKATARAMAN and B. A. DASANNACHARYA for the initiation of this subject as a thesis material and various penetrating discussions.

References

1) DAHLBORG U., FRIBERG B., LARSSON K. E. and PIRKMAJER E., Neutron Inelastic Scattering Vol. 1, 581, IAEA, Vienna (1968)
2) DE GRAAF L. A., Physica **40**, 497 (1969)
3) CHUDLEY C. T. and ELLIOT R. T., Proc. Phys. Soc. (London) **77**, 353 (1961).
4) SKÖLD K., J. Chem. Phys. **49**, 2443 (1968)
5) LECHNER R. E., ROWE J. M., SKÖLD K. and RUSH J. J., Chem. Phys. Lett. **4**, 444 (1969)
6) SCHLEMPER E. O. and HAMILTON W. C., J. Chem. Phys. **44**, 4498 (1966)
7) O'REILLEY D. E. and TASNG T., J. Chem. Phys. **46**, 1291 (1967)
8) VAN HOVE L., Phys. Rev. **95**, 249 (1954)
9) BOUTIN H. and YIP. S., Molecular Spectroscopy with Neutron, p. 48, the M. I. T. Press (1968)
10) Rush J. J. and TAYLOR T. I., Inelastic Scattering of Neutrons Vol. 2, 333, IAEA, Vienna (1965)
11) BAJOREK A., MACHECHINA T. and PARIINSKY K., Inelastic Scattering of Neutrons Vol. 2, 355, IAEA, Vienna (1965)
12) LEUNG P. S., TAYLOR T. I. and HAVENS JR W. W., J. Chem. Phys. **48**, 4912 (1968)
13) VENKATARAMAN G., USHA K., IYENGAR P. K., VIJAYARAGHAVAN P. R. and ROY A. P., J. Phys. Chem. Solids **27**, 1103 (1966)
14) STEPHENSON C. C., LANDERS L. A. and COLE A. G., J. Chem. Phys. **20**, 1044 (1952)
15) PLUMB R. C. and HORINIG D. F., J. Chem. Phys. **21**, 366 (1953)
16) RUSH J. J., TAYLOR T. I. and HAVENS W. W., J. Chem. Phys. **35**, 2265 (1961)
17) PALEVSKY H., DISCUSSION in Ref. (21)
18) VINEYARD G. H., Phy. Rev. **110**, 999 (1958)
19) WOODS A. D. B., BROCKHOUS B. N., SAKAMOTO M. and SINCLAIR R. N., Inelastic Scattering of Neutrons in Solids and Liquids, 487, IAEA, Vinna (1961)
20) VENKATARAMAN G., USHA K., IYENGAR P. K., VIJAYARAGHAVAN P. R. and ROY A. P., Inelastic Scattering of Neutrons in Solids and Liquids Vol. 2, 253, IAEA, Vienna (1963)
21) MIKKE K. and KROH A., Inelastic Scattering of Neutrons in Solids and Liquids Vol. 2, 237, IAEA, Vienna (1963)